Bioorganic & Medicinal Chemistry Letters 20 (2010) 7421–7425

Contents lists available at ScienceDirect

Bioorganic & Medicinal Chemistry Letters

journal homepage: www.elsevier.com/locate/bmcl

The discovery of tricyclic pyridone JAK2 inhibitors. Part 1: Hit to lead

Tony Siu [a,*], Ekaterina S. Kozina [a], Joon Jung [a], Craig Rosenstein [b], Anjili Mathur [c], Michael D. Altman [a], Grace Chan [b], Lin Xu [d], Eric Bachman [c], Jan-Rung Mo [c], Melaney Bouthillette [e], Thomas Rush [a], Christopher J. Dinsmore [a], C. Gary Marshall [f], Jonathan R. Young [a]

[a] Department of Chemistry, Merck & Co., 33 Avenue Louis Pasteur, Boston, MA 02115, USA
[b] Department of In Vitro Sciences, Merck & Co., 33 Avenue Louis Pasteur, Boston, MA 02115, USA
[c] Department of Pharmacology, Merck & Co., 33 Avenue Louis Pasteur, Boston, MA 02115, USA
[d] Department of Drug Metabolism, Merck & Co., 33 Avenue Louis Pasteur, Boston, MA 02115, USA
[e] Department of Basic Pharmaceutical Sciences, Merck & Co., 33 Avenue Louis Pasteur, Boston, MA 02115, USA
[f] Department of Oncology, Merck & Co., 33 Avenue Louis Pasteur, Boston, MA 02115, USA

ARTICLE INFO

Article history:
Received 24 August 2010
Revised 4 October 2010
Accepted 6 October 2010
Available online 12 October 2010

Keywords:
JAK2
Kinase
Ligand binding efficiency
Structure based design

ABSTRACT

This paper describes the discovery and design of a novel class of JAK2 inhibitors. Furthermore, we detail the optimization of a screening hit using ligand binding efficiency and log *D*. These efforts led to the identification of compound **41**, which demonstrates in vivo activity in our study.

The JAK/STAT pathway, a common signaling pathway of cytokines, regulates numerous functions of hematopoiesis and immune response including the differentiation and proliferation of cells.[1] Janus kinase 2 (JAK2) is an intracellular non receptor tyrosine kinase that belongs to the JAK family of kinases (JAK1, JAK2, JAK3, and TYK2). The presence of a catalytically inactive pseudokinase regulatory domain distinguishes the JAKs from other tyrosine kinases. Activation of JAK2 through cytokine signaling leads to phosphorylation of cytokine tyrosine residues, which serve as docking sites for signal transducers and activators of transcription (STATS). Upon binding to the receptor, the STATS are phosphorylated, then dissociated from the receptor, dimerized, and finally translocated to the nucleus for gene transcription.

Recently, the identification of the somatic mutation *JAK2*^{V617F} has demonstrated that the deregulation of JAK2 activity leads to pathogenesis of myeloproliferative disorders (MPD) including polycythemia vera (PV), essential thrombocythemia (ET), and primary myelofibrosis (PMF).[2] This clear link between gain of function mutation and pathogenesis has prompted the development of small molecule JAK2 inhibitors in the clinic as targeted therapies for myeloproliferative disorders,[3] and numerous companies have recently reported several classes of JAK inhibitors.[4] Our focus in regulating the JAK/STAT pathway has encouraged us to evaluate JAK2 inhibitors for various therapeutic areas including MPD. In this letter, we report the strategy used to develop structure activity relationships (SAR) to optimize a low micromolar screening hit into a nanomolar lead with in vivo activity.

Our strategy focused on using a virtual screening approach to rapidly identify hits and optimizing these hits utilizing rational drug design coupled with library synthesis. From the thousands of leads generated from a virtual screen,[5] compound **1** (Fig. 1) was identified as an attractive starting point to initiate chemistry. Although compound **1** has moderate activity in the in vitro JAK2 biochemical assay[6] with an IC_{50} = 1400 nM and a ligand binding

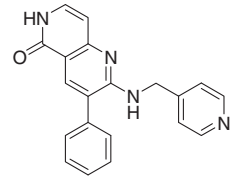

1

JAK2 IC_{50} = 1400 nM
LBE = 0.32

Figure 1. Virtual screening hit.

* Corresponding author.
E-mail address: tony_siu@merck.com (T. Siu).

0960-894X/$ - see front matter © 2010 Elsevier Ltd. All rights reserved.
doi:10.1016/j.bmcl.2010.10.031

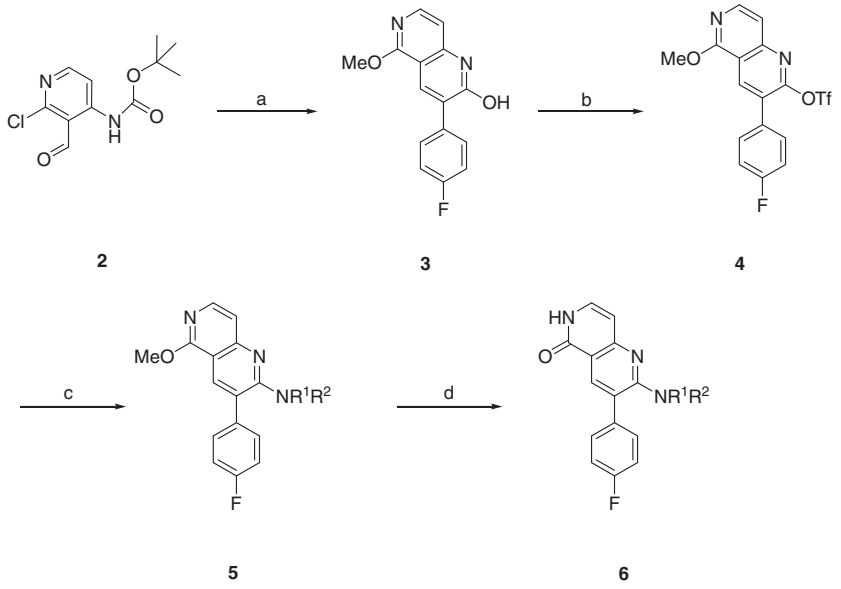

Scheme 1. Synthesis of the napthyridinone core. Reagents and conditions: (a) NaOMe (5 equiv), methyl(4-fluorophenyl)acetate, MeOH, 100 °C; (b) Cs_2CO_3, *N*-phenyl-bis(trifluoromethanesulfonimide), DMF, 0 °C; (c) NR_1R_2, dioxane, 130 °C microwave; (d) 6 M HCl/THF 80 °C.

efficiency (LBE)[7] of 0.32, it contains a novel core from which further modifications can be generated.

Novel pyridone analogs of **1** were synthesized according to the synthetic procedure in Scheme 1. Starting with known aldehyde **2**,[8] base induced cyclization with methyl(4-fluorophenyl)acetate afforded bicyclic intermediate **3**. Triflation of **3** provided **4** as an intermediate for quick analoging. Heating intermediate **4** with a variety of amines induced smooth displacement of the triflate. Subsequent hydrolysis of the methyl ether **5** under forcing acidic conditions yielded the desired pyridine compounds **6**.

Several analogs of the napthyridinone **1** were prepared according to Scheme 1. The decreased potencies of analogs **7**, **8**, and **9** (Fig. 2) as compared to **1**, suggested that further analogs made in this region of the scaffold would not significantly improve the potency. Thus, efforts were turned toward improving ligand binding efficiency by modifying the scaffold. Closer examination of structure **1** reveals that substitution of the bi-aryl portion induces a 60.5° dihedral angle conformation[9] between the bi-aryl rings. This conformation might not be optimally accommodated in the narrow ATP binding pocket of the JAK2 enzyme.[10] With this in mind, we rationalized that if the bi-aryl rings were co-planar, the proposed structure would fit better in the ATP pocket and increase potency. To test this hypothesis, two strategies were proposed to restrain conformation as shown in Scheme 2. Strategy A incorporated an intramolecular hydrogen bond as demonstrated by **10** to achieve co-planarity of **7**.[11] In principle, the intramolecular hydrogen bond between heteroatom X and the NH of the amino pyridine would induce a co-planar relationship between the ring systems. In contrast, strategy B involves achieving co-planarity and conformationally restricts **7** by fusing the rings together as depicted in **11**.

Towards this end, the approach in strategy A was adopted first due to synthetic accessibility. Using the same chemistry as shown in Scheme 1, several heteroatom variations as represented by **12**, **13**, and **14** (Fig. 3) were incorporated to induce co-planarity through intra-molecular hydrogen bonding. Unfortunately, improvements in potency using this strategy were unsuccessful. Compound **12** showed improved JAK2 activity compared to **7**. However, the ligand binding efficiency was still not in a desirable range to initiate a rapid library synthesis follow on strategy.

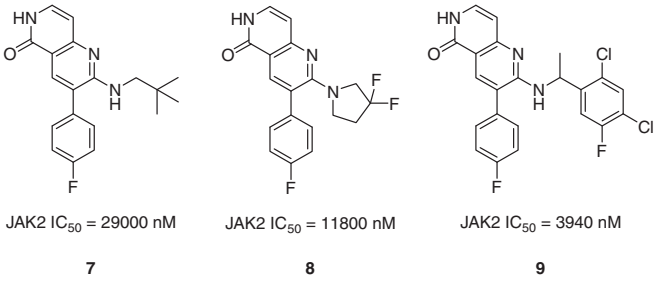

Figure 2. Activity of napthyridinone analogs.

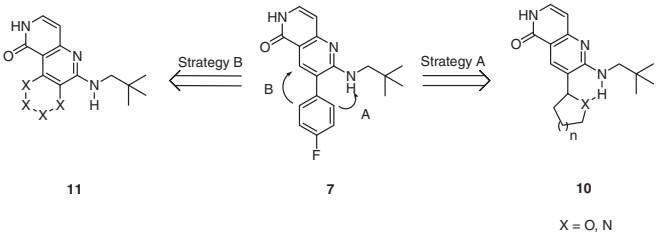

Scheme 2. Approaches to induce co-planarity of the bi-aryl rings.

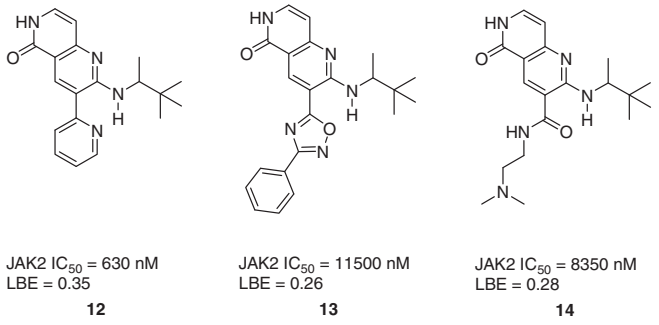

Figure 3. Intramolecular hydrogen bonding strategy.

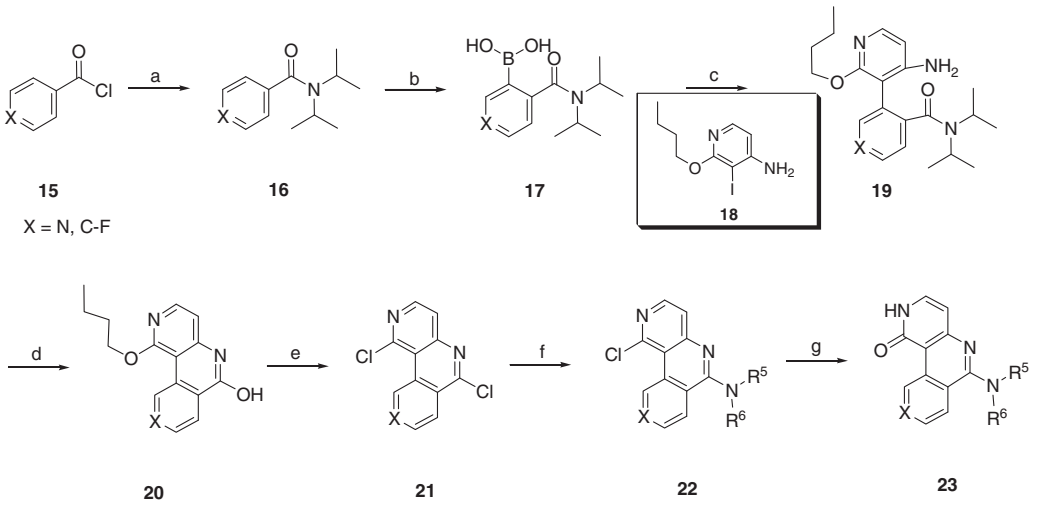

Scheme 3. Synthesis of fused napthyridinones. Reagents and conditions: (a) diisopropyl amine, triethyl amine, CH_2Cl_2; (b) *sec*-BuLi, TMEDA, triisopropylborate, THF, −78 °C; (c) **18**, $Pd(PPh_3)_4$, 2.0 M Na_2CO_3, 100 °C; (d) NaHMDS, THF, 0 °C; (e) $POCl_3$, MeCN, 100 °C; (f) amine, microwave, dioxane, 90–150 °C or LiHMDS THF 85 °C; (g) 6 N HCl dioxane, 85 °C.

Our second approach to improve intrinsic potency using strategy B required a new synthetic route that allowed for maximum diversity at a late stage in the synthesis. The construction of the tricyclic core **23** was achieved based on modification of known intermediates.[12] Acid chloride **15** was converted to the diisopropyl amide under basic conditions. Ortho lithiation of amide **16** with *sec*-butyl lithium followed by trapping with triisopropyl borate afforded the boronic acid **17**. Suzuki cross coupling of **17** with 2-butoxy-3-iodo-4-aminopyridine **18**[12] afforded bi-aryl intermediate **19**. Strong base induced ring closure with NaHMDS gave the tricyclic core **20**. Heating tricyclic **20** in $POCl_3$ resulted in the double chlorination to provide intermediate **21**. A variety of amines added to the core either via thermally or microwave induced reactions at high temperature with acid or base. Interestingly, the subtle difference in reactivity of the two chlorines allows for selective substitution. In the majority of cases, the amine added to **21** to provide the desired regioisomer as shown in **22**.[13] Finally, selective hydrolysis of intermediate **22** provided pyridone **23**.

With the synthesis to form fused scaffold **11** in hand, compound **24** was prepared first to test our original hypothesis of co-planarity. To our delight, compound **24** (Scheme 4) improved the intrinsic potency 1000-fold (JAK2 IC_{50} = 26 nM) compared to compound **7** (JAK2 IC_{50} = 29000 nM), confirming the feasibility of our approach. Furthermore, significant gains were made in ligand binding efficiency for **24** (LBE = 0.45) compared to **7** (LBE = 0.26).

Encouraged by the potency enhancement and gains in ligand binding efficiency, **24** was used as a frame of reference for probing structure–activity relationships (SAR) of a diverse subset of amines. Table 1 highlights the in vitro data of amine analogs that were synthesized. The focus for this amine library centered on improving potency as well as understanding the structural environment in this region of the enzyme. Polar substituents, especially with basic amines such as in examples **25** and **27**, are examined in this region of the kinase, but are not well tolerated. Secondary amines, such as **29**, are tolerated, but did not improve potency compared to **24**. Interestingly, aniline **30** is only moderately active with IC_{50} = 4100 nM; however, the activity is dramatically improved when ortho substituents are incorporated as exemplified by **31** (IC_{50} = 4 nM) and **32** (IC_{50} = 14 nM). This result suggests that the strong conformational preference for the aniline ring to adopt a perpendicular conformation to the core significantly contributes to the binding affinity. Furthermore, larger hydrophobic groups such as **33** are active, suggesting size tolerability in this area of the kinase pocket.

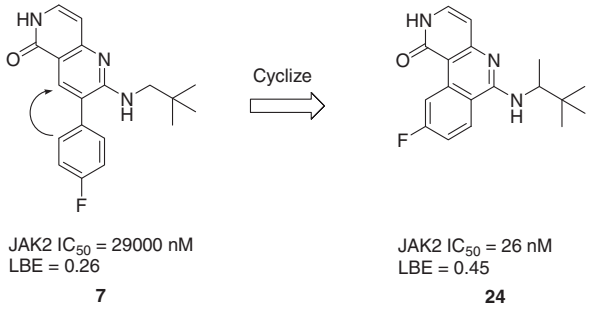

Scheme 4. Strategy B for improving potency.

Substitution with smaller hydrophobic amines branched at the alpha positions such as **34**, **35**, and **36** trends toward improvements in potency when compared to larger hydrophobic amines. Most notable is **38** with a JAK2 IC_{50} = 1 nM. Remarkably, **38** is 27-fold more potent than its methyl analog **36**, underscoring the crucial contribution that the trifluoromethyl substituent makes with the JAK2 enzyme. The enantiomer **39** is significantly less active with an IC_{50} = 55 nM. Due to its excellent potency and efficient binding (LBE = 0.49), **38** was advanced for further investigation.

To better understand how our inhibitors bind to the enzyme, compound **38** was modeled into the JAK2 crystal structure.[14] As shown in Figure 4, compound **38** is proposed to bind in the ATP binding pocket of JAK2 with the pyridone interacting with the hinge region of the kinase. The pyridone makes critical H-bonds to the backbone carbonyl of Glu930 and backbone NH of Leu932. The planar structure nicely fits into the narrow ATP binding pocket along the hinge, which may account for a significant proportion of the potency. Furthermore, the amine linkage is proposed to occupy the ribose pocket of the enzyme. More specifically, the CF_3 moiety is positioned into a hydrophobic pocket formed by Leu983 and Gly993. The increased lipophilicity of the CF_3 group interacting with the hydrophobic pocket seems to explain the increased potency compared to the methyl analog (**36**). The fluorine substituent on the aromatic ring, however, does not interact with the protein and is projected out into solvent.

Table 1
SAR on fused napthyridinone analogs

R	Enzyme IC_{50} (nM) JAK2	R	Enzyme IC_{50} (nM) JAK2
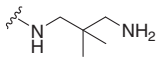 **25**	3157	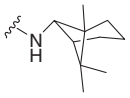 **33**	200
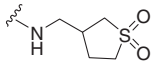 **26**	512	 **34**	75
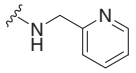 **27**	1115	 **35**	139
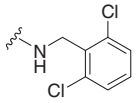 **28**	53	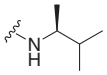 **36**	27
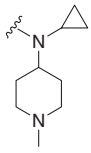 **29**	540	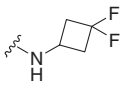 **37**	750
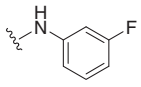 **30**	4100	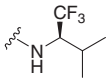 **38**	1
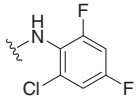 **31**	4	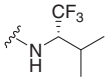 **39**	55
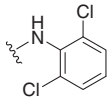 **32**	14	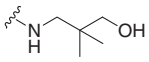 **40**	274

Having optimized the intrinsic potency, compound **38** was further profiled to understand the liabilities associated with this compound (Table 2). In addition to having excellent enzymatic potency, **38** demonstrates good activity in our cell based assay JAK2 Cell IC_{50} = 50 nM.[15] Further investigation in vivo revealed modest pharmacokinetic properties in rat with a Cl = 21 mL/min/kg and Vd = 6 L/kg.[16] However, a liability of **38** is the off-target binding affinity to the I_{kr} potassium channel hERG (human Ether-a-go-go-Related Gene) with IC_{50} = 3500 nM.[17] Moreover, while quite potent, **38** suffers from poor aqueous solubility as measured in our solubility assay. Unfortunately, the reduced solubility limited in vivo studies with **38**, and a strategy to improve aqueous solubility while maintaining the potency was needed.

Based on our modeling study, the trajectory of the aryl fluoride substituent of **38** is pointing away toward the open end of the catalytic site and into solvent. Consequently, the incorporation of polar functional groups in this region of the molecule to modify physicochemical properties without affecting the potency would be a viable strategy. Towards that end, compound **41** incorporating a nitrogen heteroatom was synthesized according to Scheme 3. As

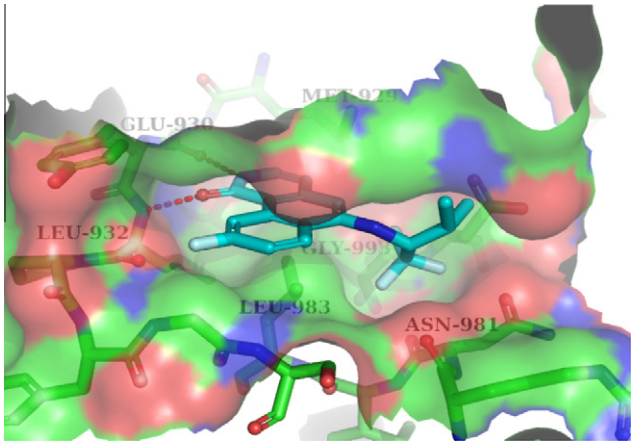

Figure 4. Proposed binding mode of compound **38** bound to JAK2 X-ray structure.

predicted, the incorporation of this nitrogen reduces the experimental HPLC log *D* from 3.34 to 2.33,[18] and the HCl salt of **41** has aqueous solubility up to 120 μM in a solubility assay. Furthermore, the activities in both the enzymatic and cell based assays are maintained, validating the hypothesis for modifying physicochemical properties without diminishing potency. In addition, as an added benefit, incorporating the polar heteroatom decreases the hERG binding.[19] However, the lower log *D* diminishes the pharmacokinetic properties of **41** with a Cl = 68 mL/min/kg. Nevertheless, on the basis of the excellent intrinsic and cellular potency coupled with improved aqueous solubility, **41** was evaluated in an in vivo model.[20] Administration of **41** at doses of 30 and 90 mpk (p.o.) reduces pSTAT5 signals to basal levels in whole blood of erythropoietin (Epo) treated mice at 1 and 3 h (Fig. 5), with an IC_{50} = 2700 nM.[21]

In conclusion, low micromolar focused screening hit **1** was optimized by rational targeted design along with diversity oriented synthesis using ligand binding efficiency as a guiding parameter for optimization. We were able to identify **38** as a lead, improving the potency by 1400-fold while enhancing the ligand binding efficiency to 0.49. With the aid of molecular modeling, judicious introduction of a polar functionality led to **41**, which reduces hERG binding and increases aqueous solubility. Compound **41** potently reduces pSTAT5 levels in mice and allowed us to achieve in vivo proof of concept. The detailed optimization of the pharmacokinetic properties and in vivo potency of **41** will be disclosed in a future communication.

Table 2
Profile of compound **38** and **41**

	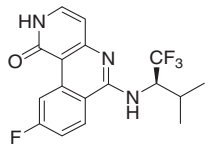 **38**	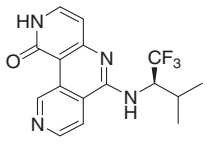 **41**
JAK2 (IC_{50})	1 nM	1 nM
Cell (IC_{50})	50 nM	40 nM
hERG (IC_{50})	3500 nM	1400 nM
Rat Cl_p	21 mL/min/kg	68 mL/min/kg
V_D	6 L/kg	8 L/kg
HPLC log *D* pH 7.4	3.34	2.33
Solubility @ pH 7	3 μM	120 μM
In vivo IC_{50}	NA	2700 nM

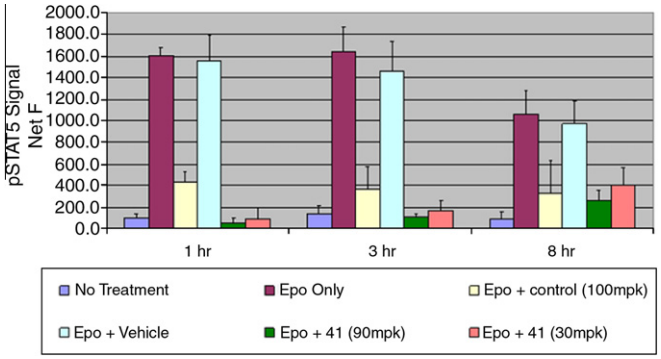

Figure 5. Inhibition of pSTAT5 signal in C57Bl/6 mice ($n = 6$) by oral dosing of compound **41** at 30 and 90 mpk.

Acknowledgments

T.S. thanks Christopher Cox, Lily Moy, and Kerrie Spencer for careful reading of this manuscript and Bruce Adams for NMR support.

References and notes

1. Shuai, K.; Liu, B. *Nat. Rev. Immunol.* **2003**, *3*, 900.
2. (a) James, C.; Ugo, V.; Le Coudeic, J. P.; Staerk, J.; Delhommeau, F.; Lacout, C.; Garcon, L.; Raslova, H.; Berger, R.; Bennacaur-Griscelli, A.; Villeval, J. L.; Constantinescu, S. N.; Casadevall, N.; Vainchenker, W. *Nature* **2005**, *434*, 1144; (b) Baxter, E. J.; Scott, L. M.; Campebell, P. J.; East, C.; Fourouclas, N.; Swanton, S.; Vassiliou, G. S.; Bench, A. J.; Boyd, E. M.; Curtin, N.; Scott, M. A.; Erber, W. N.; Green, A. R. *Lancet* **2005**, *365*, 1054; (c) Levine, R. L.; Wadleigh, M.; Cools, J.; Ebert, B. L.; Wernig, G.; Huntly, B. J. P.; Boggon, T. J.; Wlodarska, I.; Clark, J. J.; Moore, S.; Adelsperger, J.; Koo, S.; Lee, J-C.; Gabriel, S.; Mercher, T.; D'Andrea, A.; Frohling, S.; Dohner, K.; Marynen, P.; Vandenberghe, P.; Mesa, R. A.; Tefferi, A.; Griffine, J. D.; Eck, M. J.; Sellers, W. R.; Meyerson, M.; Golub, T. R.; Lee, S. J.; Gilliland, D. G. *Cancer Cell* **2005**, *7*, 387.
3. (a) Fridman, J.; Nussenzveig, R.; Liu, P.; Rodgers, J.; Burn, T.; Haley, P.; Scherle, P.; Newton, R.; Hollis, G.; Freidman, S.; Verstovsek, S.; Vaddi, K. *Blood*, ASH Annual Meeting Abstracts, 2007, *Abstr. 110*, 3538.; (b) Verstovsek, S.; Pardanani, A. D.; Shah, N. P.; Sokot, L.; Wadleigh, M.; Gilliland, D. G.; List, A. F.; Tefferi, A.; Kantarjian, H. M.; Bui, L. A.; Clary, D. O. *Blood* ASH Annual Meeting Abstracts, 2007, *Abstr. 110*, 553.; (c) Geron, I.; Abrahamsson, A. E.; Barraoga, C. F.; Kavalerchik, E.; Gotlib, J.; Hood, J. D.; Durocher, J.; Mak, C. C.; Noronha, G.; Soll, R. M.; Tefferi, A.; Kaushansky, K.; Catriona, K.; Jamieson, C. H. M. *Cancer Cell* **2008**, *13*, 321.
4. Wilson, L. J. *Expert Opin. Ther. Pat.* **2010**, *5*, 609.
5. A virtual screen was performed to identify molecules in Merck's collection that would be predicted to bind to the ATP binding pocket of JAK2 (PDB ID: 2B7A). The GLIDE docking software from Schrodinger was run in parallel mode against structures of JAK2 with and without water molecules bound to the active site. The best scoring hits were visually inspected, and the most interesting and novel molecules were chosen for experimental follow-up.
6. Detection of peptide phosphorylation was performed by homogenous time resolved fluorescence (HTRF) using a europium chelate. IC_{50} values are reported as the averages of at least two independent determinations; standard deviations are within ±25–50% of IC_{50} values. For further details see: WO2009035575.
7. (a) Abad-Zapatero, C. *Expert Opin. Drug Disc.* **2007**, *2*, 469; (b) Hopkins, A. L.; Groom, C. R.; Alex, A. *Drug Discov. Today* **2004**, *9*, 430.
8. Siu, T.; Liang, J.; Arruda, J.; Li, Y.; Jones, R. E.; Defeo-Jones, D.; Barnett, S. F.; Robinson, R. G. *Bioorg. Med. Chem. Lett.* **2008**, *18*, 4186.
9. Conformational analysis was performed with Macromodel module from Schrodinger, LLC. Mixed torsional/low-mode sampling algorithm was used to generate conformers with OPLS-2005 force field and implicit solvent model. To ensure sufficient sampling, the maximum energy cutoff was set at 8 kcal/mol.
10. X-ray structure of JAK2 (PDB ID: 2B7A)
11. Kuhn, B.; Mohr, P.; Stahl, M. *J. Med. Chem.* **2010**, *53*, 2601.
12. Rodgers, J. D; Robinson D. J.; Arvanitis, A. G.; Maduskuie, T. P. Jr.; Shepard, S.; Storace, L.; Wang, H.; Rafalski, M.; Jalluri, R. K.; Combs, A. P.; Crwely, M. L. Preparation of tetracyclic inhibitors of Janus kinases for treating immune-related diseases and cancer. PCT Int. Appl. WO2005105814, 2005.
13. The structure was determined by observing the nOe interaction between the N–H and aromatic proton H^1 in the ^1H NMR spectrum.

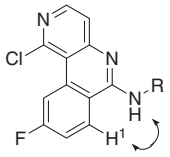

14. Docking studies were performed using Glide software from Schrodinger, LLC. Based on the X-ray structure of JAK2 (PDB ID: 2B7A). Extra precision mode (XP) with default settings were used to generate 20 docked poses which were subsequently filtered based on visual inspection.
15. Detection of STAT phosphorylation was performed using AlphaScreen™ SureFire™ p-STAT5 assay (Perkin–Elmer and TGR Biosciences) using both biotinylated anti-phospho-STAT5 antibody, which is captured by Streptavidin-coated donor beads, and anti-total STAT5 antibody, which is captured by Protein A conjugated acceptor beads. IC_{50} values are reported as the averages of at least two independent determinations; standard deviations are within ±25−50% of IC_{50} values. For further details see: WO2008156726.
16. Dosed in Sprague–Dawley rats ($n = 1$) IV 1 mg/kg as 1 mg/mL solution PEG400:Captisol (1:1).
17. The hERG IC_{50} values were acquired by radioligand binding competition experiments using membrane preparations from human embryonic kidney cells that express hERG. IC_{50} values are reported as the averages of at least two independent determinations; standard deviations are within ±25–50% of IC_{50} values. For assay detail see Bell, I. M.; Gallicchio, S. N.; Abrams, M.; Beshore, D. C.; Buser, C. A.; Culberson, J. C.; Davide, J.; Ellis-Hutchings, M.; Fernandes, C.; Gibbs, J. B.; Graham, S. L.; Hartman, G. D.; Heimbrook, D. C.; Homnick, C. F.; Huff, J. R.; Kassahun, K.; Koblan, K. S.; Kohl, N. E.; Lobell, R. B.; Lynch, J. J., Jr.; Miller, P. A.; Omer, C. A.; Rodrigues, A. D.; Walsh, E. S.; Williams, T. M. *J. Med. Chem.* **2001**, *44*, 2933. and references therein.
18. Waring, M. J. *Expert Opin. Drug Disc.* **2010**, *5*, 235.
19. Siu, T.; Li, Y.; Nagasawa, J.; Liang, J.; Tehrani, L.; Chua, P.; Jones, R. E.; Defeo-Jones, D.; Barnett, S. F.; Robinson, R. G. *Bioorg. Med. Chem.* **2008**, *18*, 4191.
20. Mathur, A.; Mo, J.; Kraus, M.; O'Hare, E.; Sinclair, P.; Young, J.; Zhao, S.; Wang, Y.; Kopinja, J.; Qu, X.; Reilly, J.; Walker, D.; Xu, L.; Aleksandrowicz, D.; Marshall, G.; Scott, M. L.; Kohl, N. E.; Bachman, E. *Biochem. Pharmacol.* **2009**, *78*, 382.
21. Compound **41** was dosed by oral gavage to C56bl/6 mice as a solution in 40%PEG400: 50%Trappsol: 10% water. Drug concentrations and pSTAT5 signal were measured at 1, 3, and 8 h.